Geomechanics and Engineering, *Vol. 9, No. 2 (2015) 243-259*
DOI: http://dx.doi.org/10.12989/gae.2015.9.2.243

Comparative study on the behavior of soil fills on rigid acrylic and flexible geotextile containers

Hyeong-Joo Kim [1a], Myoung-Soo Won [1b], Jang-Baek Lee [2c], Jong-Hoon Joo [2d] and Jay C. Jamin [*2]

[1] *Department of Civil Engineering, Kunsan National University, Gunsan 573-701, Republic of Korea*
[2] *School of Civil and Environmental Engineering, Kunsan National University, Gunsan 573-701, Republic of Korea*

(*Received April 28, 2015, Revised June 10, 2015, Accepted June 24, 2015*)

Abstract. Comparative study has been performed to investigate the behavior of dredged fills on rigid (Model 1) and flexible (Model 2) containers. The study was focused on the sedimentation of soil fills and the development of total stresses. Model 1 is made of an acrylic cylinder and Model two is a scale-size geotextile tube. Results indicate that for rigid containers, significant decrease of the sediment height is apparent during the dewatering process. On the other hand, because the geotextile is permeable, the water is gradually dissipated during the filling process on flexible containers. Hence, significant loss in the tube height is not apparent during the duration of the test. Pressure spikes are apparent on rigid containers during the filling process which can be attributed to the confining effect due to hydrostatic pressure. For the flexible containers, the pressure readings gradually increases with time during the filling process and normalize at the end on the filling stage. No pressure spikes were apparent due to the gradual dissipation of pore water pressure.

Keywords: rigid container; flexible container; total stress; geotextile strain; model test

1. Introduction

Geotextile tubes are widely used in South Korea since the late 1990s up to the present. Presently, the annual consumption of cement and concrete has significantly increased in South Korea. There is a decreasing supply of cement and construction aggregates such as rock, gravel and sand whose quantities are now limited due to environmental restrictions in the quarry site. Construction expenses have also increased due to additional delivery costs from source to site and construction time is longer due to may process and equipment involved. Geotextile tube technology could be a viable alternative to the conventional ruble mound structures in cases where temporary protection is required or rock is not obtainable and difficult to transport to the site.

Geotextile tubes are made from strong and flexible textile materials that are capable of

*Corresponding author, Ph.D. Student, E-mail: jaminjc@kunsan.ac.kr
[a] Ph.D., Professor, E-mail: kimhj@kunsan.ac.kr
[b] Ph.D. Assistant-Professor, E-mail: wondain@kunsan.ac.kr
[c] Ph.D. student, E-mail: leejb@kunsan.ac.kr
[d] Graduate student, E-mail: honix@kunsan.ac.kr

 ISSN: 2005-307X (Print), 2092-6219 (Online)

retaining fine-grained materials though permeable enough to allow the excess water from the hydraulically filled slurry to dissipate. In recent years geotextile tubes were used as groins and breakwaters to protect or mitigate shoreline/coastline erosions (Cantré 2002, Gibeaut *et al*. 2003, Alvarez *et al*. 2007, Pilarczyk 2008, Parab *et al*. 2011), as containment dikes for land reclamation and man-made islands (Fowler *et al*. 2002a, b), and as revetments acting as mass-gravity barrier-type structures and protection dikes to prevent damage to valuable structures caused by natural calamities (Restall *et al*. 2002, Lawson 2008).

Geotextile tubes has been of interest in various studies due to its wide applications in civil engineering. Laboratory evaluation results on the permeability and retention characteristics of geotextiles can be found in the studies of Moo-Young *et al*. (2002), Koerner and Koerner (2006), Weggel *et al*. (2011) and Vashi *et al*. (2013). Model tests and large-scale experiments on geotextile tubes can be found in the literature (Recio and Oumeraci 2009, Kriel 2012, Kim *et al*. 2013b, 2014a, b). Numerical (Kim *et al*. 2013a, 2014b) & analytical methods (Plaut and Klusman 1999) were also conducted to study the stability of stacked geotextile tubes. In general the studies available in the literature focuses on the investigation of the hydraulic stability of stacked geotextile tubes and the geotextile performance in strength, durability and permeability. However, very little is presently understood about the consolidation behavior of the fill materials and the stress and strain behavior of the confining geotextile. Brink *et al*. (2013, 2015) has proposed a consolidation modeling method for geotextile tubes filled with fine-grained materials. Cantré and Saathoff (2011) has numerically formulated a design method for tubes considering the geotextile strain.

A comparative study have been performed to investigate the behavior of dredged fills on rigid and flexible containers. The study was focused on the sedimentation of slurry fill and the development of total stresses induced by the dewatered fill material. The procedures and results are presented in the following sections.

2. Material properties and instrumentation

2.1 Dredged fill properties

The model test have been carried out at the geotechnical engineering laboratory at Kunsan National University. The fill material was obtained from a local dredging site in the Saemangeum river estuary near Gunsan City. The physical properties of the dredged fill are shown in Table 1 and its gradation curve is given in Fig. 1.

Table 1 Dredged fill properties

Item	Quantity
Natural water content, ω_n (%)	15.9
Specific gravity of soil solids, G_s	2.69
Plasticity Index, *PI* (%)	N.P.*
Percent passing #200 sieve	25
Soil classification (USCS)	SM**

*non-plastic; **silty-sand

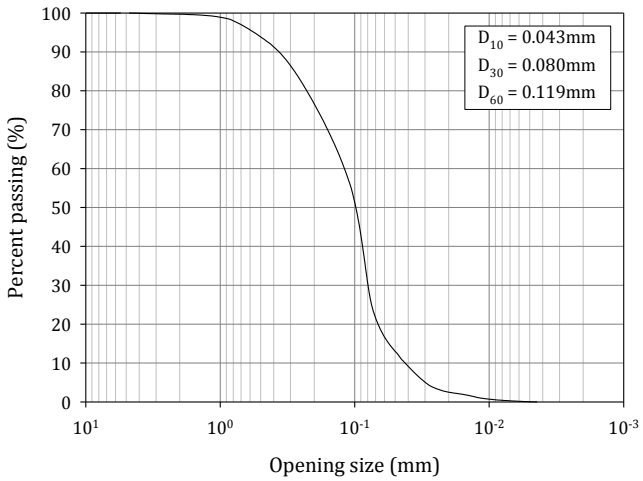

Fig. 1 Gradation curve

Table 2 Woven geotextile properties

Description/Unit	Quality/Quantity
Material type	P.P.*
Thickness (mm)	2.0
Tensile strength	
Longitudinal	195
Transverse	180

*Polypropylene

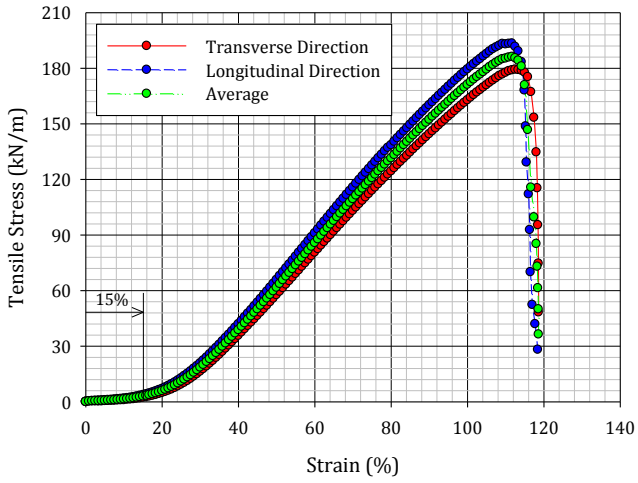

Fig. 2 P.P. Geotextile tensile stress-strain curve

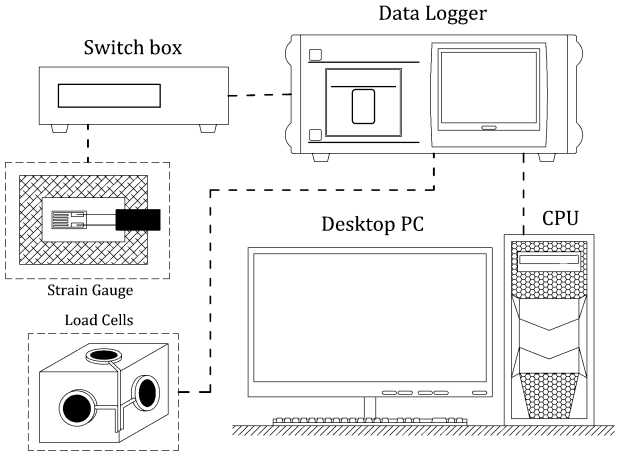

Fig. 3 Data station

2.2 Geotextile properties

The geotextile tube used in the present study is made of a woven P.P. (polypropylene) geotextile material. The geotextile tube is 4.0 m long and has a theoretical diameter of 1.0 m. The physical properties of the geotextile tube are shown in Table 2. The geotextile tensile strength-strain relationship obtained from a laboratory test of the P.P. material is shown in Fig. 2. Initially the polypropylene geotextile is strained up to 15% with minimal force. This can be attributed to the realignment of loose geotextile fibers at start of the application of the tensile force.

2.3 Instrumentation

In this study, total stress transducers (TST) and strain gauges (SG) were used to monitor the development of stress and strain during the experiment. All the measurement data are stored and interpreted by a desktop computer. The schematic of the data station is shown in Fig. 3.

3. Laboratory setup and procedure

3.1 Model 1: *Acrylic cylinder* (*Rigid container*)

Fig. 4 illustrates the schematic diagram of the apparatus used for Model 1 test. The laboratory setup shown in Fig. 4(a) comprises of a mixing tank, gravity tank or the elevated tank, and the acrylic cylinder. The mixing and gravity tanks are equipped with electric driven agitators used for the mixing of the water-soil mixture. The detail for the acrylic cylinder is shown in Fig. 4(b). The acrylic cylinder's filling port is located on the center. Measurement points/sections for the height of accumulated soils are located at ①, ②, ③, ④, ⑤, ⑥, ⑦, ⑧, and ⑨, as shown in Fig. 4(b). The TST contraption shown in Fig. 4(c) are located at Ⓐ and Ⓑ.

The slurry is prepared in the mixing tank where water and dredged soil are combined and is constantly agitated with an electric agitator. After the desired slurry consistency is reached the

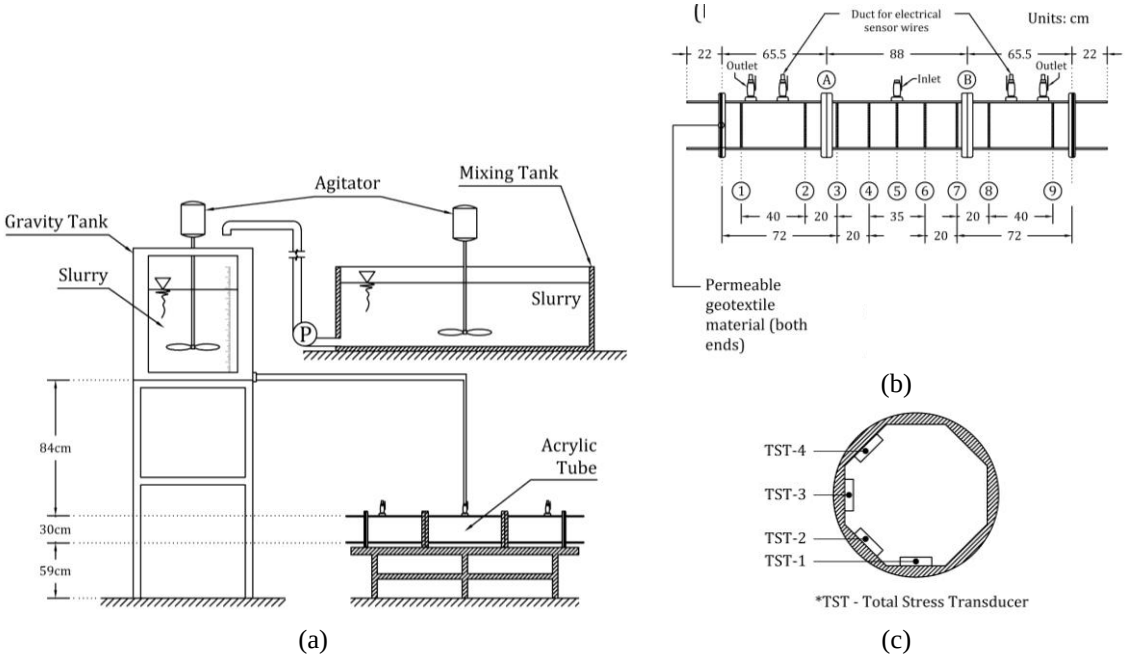

Fig. 4 (a) Model 1 laboratory setup; (b) acrylic cylinder detail; and (c) total pressure transducer (TST) placement

soil-water mixture is hydraulically pump to the gravity tank. An electric agitator is also provided in the gravity tank to maintain the slurry consistency.

Initially the plan was to fill the geo-cylinder continually until the tube a maximum soil height deposit is achieved (usually at the inlet of the tube, where filling becomes impossible due to the soil deposits blocking the inlet). However, in the case of the present study, the filling process was hindered by the rapid accumulation of filter cake on the permeable geotextiles at the ends of the tube. Hence it was decided to fill the tube more than once.

3.2 Model 2: *Geotextile tube* (*Flexible container*)

The large-scale apparatus shown in Fig. 5 is equipped with a mixing station, pumping and delivery station, and an observation station. The mixing station comprises of a ① mixing tank and ② water supply tank. Soil (Dredged soil or sand) and water are combined in the mixing tank for the slurry preparation. An electric agitator composed of a shaft rod attached to an electric motor at one end and an impeller at the other end is installed above the mixing tank. The electric agitator blends the soil and water mixture until a slurry material is produced. In the pumping and delivery station a ③ hydraulic pump is used to draw the slurry from the mixing tank via the ④ two-way slurry delivery pipe system during the filling process. There are two filling options for the slurry into the geotextile tube, through direct hydraulic pumping or via the ⑤ gravity tank. For the hydraulic filling, the slurry is hydraulically pumped into the geotextile tube. Alternatively, geotextile filling by gravity initially requires pumping the slurry from the mixing tank to the gravity tank. An electric agitator is also installed on top of the gravity tank to continually agitate

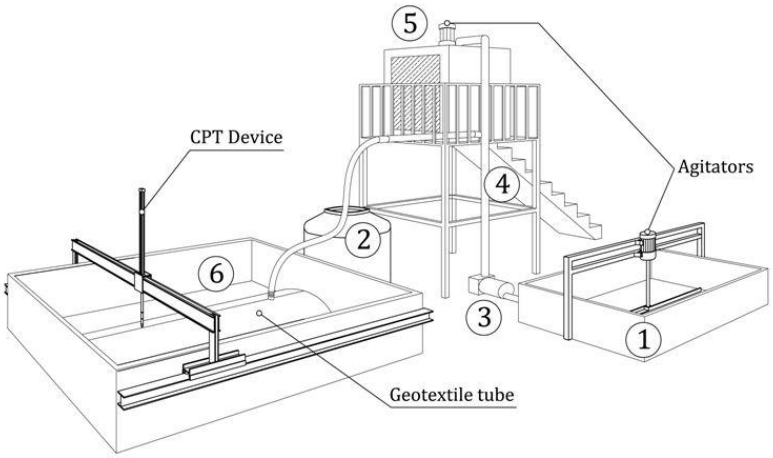

Fig. 5 Model 2 experiment setup

the slurry mixture. To fill the geotextile tube, a gate valve at the bottom of the tank is opened and the slurry is filled through gravitation. In the case of gravity filling, the pumping pressure will be based on the hydraulic head of the slurry in the gravity tank. The hydraulic head will be equal to the difference between the elevation of the filling port and the elevation of the slurry surface. For the present study, the geotextile tubes were filled hydraulically. The experimental observations for the geotextile tube models are made in the observation station or the ⑥ test tank. The steel tank floor have dimensions of 3 m × 5 m and can be filled with water at a maximum height of 1.5 meters to simulate geotextile tube models under submerged conditions. In both submerged and non-submerged geotextile tube test cases, water from the test tank can be recycled and reused for the next experiment by pumping out the water back to the water supply tank using submersible water pumps.

Strain gauges are also placed on the outer skin of the geotextile. Details for the location and placement of the pressure and strain sensors are shown in Fig. 6. The strain gauge and pressure cell readings were collected by the data logger and interpreted by a desktop computer in the data station. The strain gauge is attached to the geotextile skin in the same manner shown in Fig. 6(a) along the transverse direction of the tube to measure the tube's circumferential strain. The

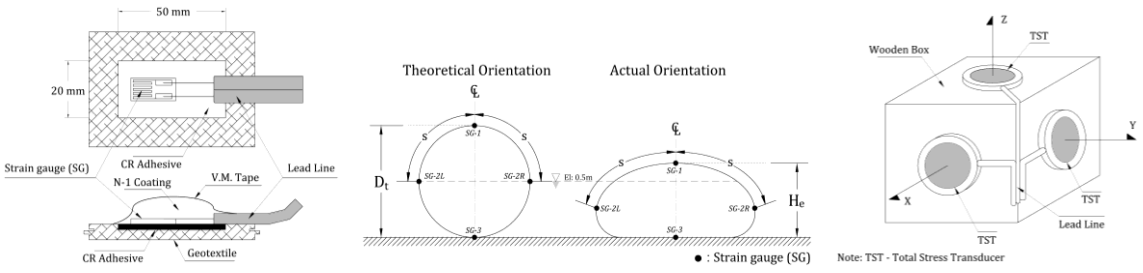

(a) (b) (c)

Fig. 6 (a) Strain gauge installation details; (b) strain gauge positioning on the geotextile tube, and; (c) total stress transducer contraption

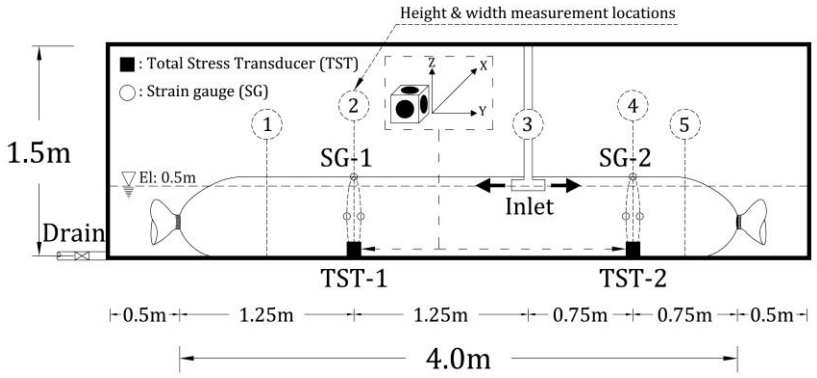

Fig. 7 Model 2 instrumentation placement

surface of the geotextile area where the strain gauge will be attached should be cleaned. Then a sufficient amount of chloroprene (CR) adhesive (occupies at least about an area of 20 mm × 50 mm) is spread on the surface of the geotextile skin. The strain gauge is then placed on top of the applied CR adhesive. After the strain gauge is secured, an N-1 coating is coated on top of the strain gauge to cover the device. Lastly, the attachment is covered with a VM tape for water proofing. In this study, four strain gauges were attached to the tube in the same manner as shown in Fig. 6(b). The section in the geotextile tube where the strain gauges are placed is shown in Fig. 7.

For the slurry preparation, the dredged soil and water are combined in the mixing tank. A 3:1 water to soil ratio slurry mixture (300% water content) is used for both geotextile tube experiments. The mixture was continually stirred by the electric agitator to achieve an even mixture and retain the desired slurry consistency. Concurrent with the slurry preparation, the geotextile tube is placed into position inside the test tank. The geotextile tube is filled hydraulically. The slurry is pumped into the geotextile tube through the improvised T-type inlet system during the filling phase. The tubes are filled, dewatered and refilled again until the dewatered height of the tube following the last filling phase is approximately equal to 40~50% the theoretical diameter of the geotextile tube. The pumping pressure during filling was maintained at 30 kN/m^2. Measurements of the tube height and width at each section are taken after filling (filled height & width) and before refilling (dewatered height & width) of slurry. The strain and pressure data are collected via a data logger and monitored through a desktop PC (Fig. 3). After the filling and dewatering tests, soil samples were gathered from the topmost and bottom part of the tube. The water content and percent passing #200 sieve of these samples were determined to evaluate the variation of fill material characteristics in the tube.

4. Test results

4.1 Accumulated soil height

The recorded measurements for the accumulated soil fill on Model 1 is shown in Fig. 8(a) and the progress of the filled tube height of Model 2 is shown in Fig. 8(b). The filling rates for Models 1 & 2 were methodically kept at constant during the each test. Model 1 was initial planned to

hydraulically filled (though gravity force) with slurry at Q_1 = 0.0106 m^3/min. The measured pumping pressure was approximately 18 kPa during the entire experiment. The slurry material was injected into the tube at water content ω = 300%. The first filling stage lasted for approximately 80 min. Ten minutes after the first filling, clogging due to the accumulation of filter cakes on both the geotextile sheet covers at the ends of the cylinder occurred. In consequence, the filling rate was reduced at this point and the deposition of soil sediments became gradual. The tube inlet was closed at time t = 80 min and was allowed to dewater for approximately 20 min. At this stage the settlements at Locations A and B became apparent. At t = 100, the tube was pumped again with slurry. This time, the two outlets for drainage at the top of the cylinder were kept opened to allow drainage of the excess water (since at this point, seepage flow though the geotextile sheets became sluggish). At this point, it can be seen then the deposited soil height at Locations A and B doesn't change at all. This seems to be unlikely. However, looking at Fig. 9, it can be seen that the soil height at sections ①, ②, ④, ⑤, ⑥, ⑧, and ⑨ were changing with time. Negligible changes for the soil height occurs at sections 3 and 7 (Location A and B). This could be attributed to the type of inlet system (T-shaped inlet system) used during the test. It might be that during filling, due to the shape of the inlet system, the soil particles were transported at longer distances (i.e., sections ①, ②, ⑧ and ⑨), as suggested from the measurement data shown graphically in Fig. 9.

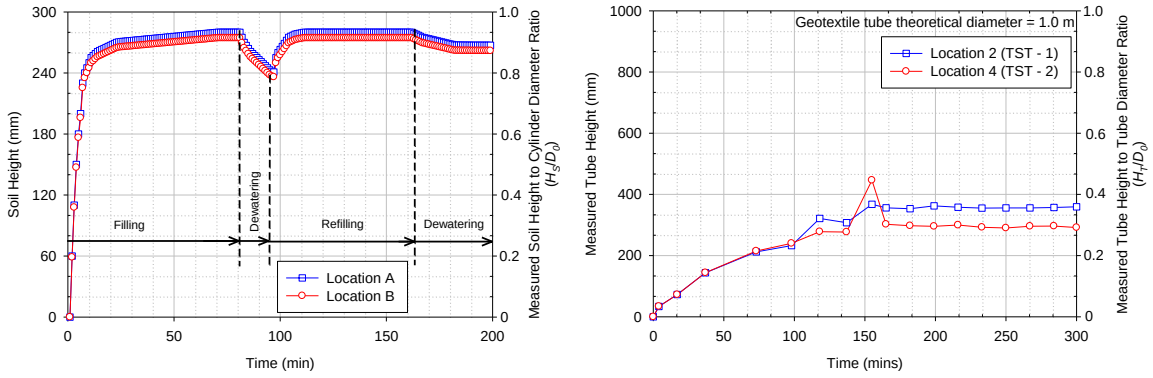

(a) (b)

Fig. 8 Non-dimensional soil height: (a) Model 1; (b) Model 2

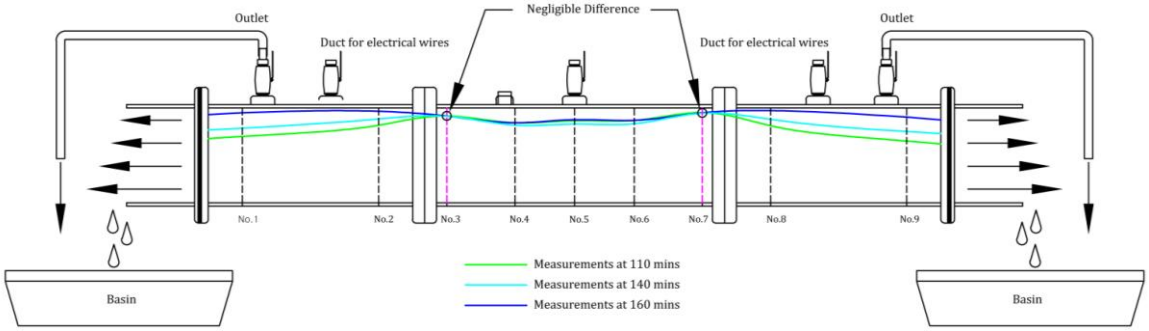

Fig. 9 Accumulation of soil during filling of Model 1

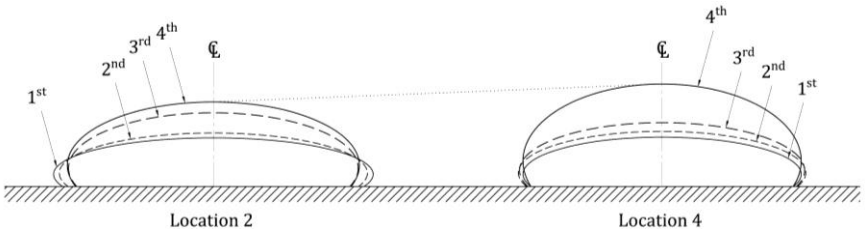

(a)

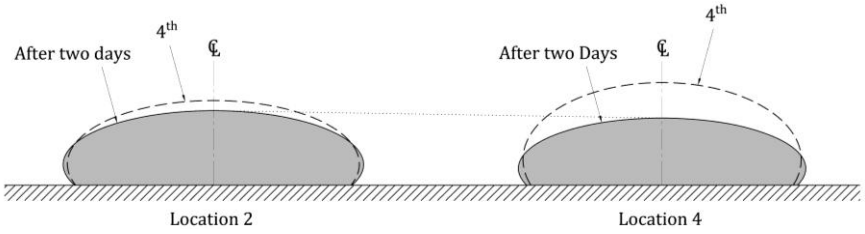

(b)

Fig. 10 Geotextile tube shape variation: (a) during filling stages; (b) stabilized stage – two days after the last filling stage

Table 3 Summary of the variation in the geotextile tube's shape properties

Description	Property	Filling stage				Stabilized stage (after two days)
		1st	2nd	3rd	4th	
Location 2	Height (mm)	212	233	321	368	360
	Width (mm)	1390	1340	1260	1265	1260
Location 4	Height (mm)	215	240	278	446	292
	Width (mm)	1210	1250	1240	1205	1245

Model 2 was hydraulically pumped with slurry (ω = 300%) at Q_2 = 0.0681 m^3/min at an average pumping pressure (P_0) = 32.96 kPa. The hydraulic pump has a maximum pumping power of 5 HP. In this experiment, four filling stages were conducted for the geotextile tube model. The slurry pumping were conducted at t_1 = 0 min, t_2 = 40 min, t_3 = 90 min and t_4 = 150 min. Each filling stages were approximately 10-15 min. Model 2 displays a different type of behavior during the filling process. Because the geotextile is permeable, the water is gradually dissipated during the filling process. Hence, no significant loss in the tube height is apparent during the test. Fig. 10 illustrates the variation of the tube sections at Locations ② and ④ (please refer to Fig. 7) and the corresponding tube height and width for each stage are tabulated in Table 3. Evidently the tube height in both sections varies after each filling stage. The variation in the tube height and width can be attributed to the water content and percentages of fine deposits in the area. Laboratory tests on the soil samples, obtained from Locations ② and ④ after the filling and dewatering tests, indicates that Location ② contains less amount of fine particles (17%) and water content (16%) compared to Location ④ where the fine particles are about 25% having a moisture content of about 36%. This also explains why a significant drop in tube height occurred in Location ④, two days after the last filling stage, as shown in Fig. 10(b).

4.2 Total stress development

4.2.1 Model 1

The total pressure readings for Model 1 are shown in Fig. 11 (for the placement and orientation of these devices in the cylinder, please refer to Fig. 4). The readings for the pressure transducers at Locations Ⓐ and Ⓑ are exhibited at Figs. 11(a) and (b), respectively. The pore water pressure readings is shown in Fig. 12(a). The effective horizontal and vertical stresses at Locations Ⓐ and Ⓑ are illustrated in Fig. 12(b). The recorded pressures for Model 1 clearly reflects the hydrostatic pressure from the gravity tank. As mentioned earlier, the measured pumping pressure was 18 kPa. The average total stresses during the 1st & 2nd filling, and during the final dewatering stages acting on the acrylic cylinder wall were plotted and shown in Fig, 13(a). It can be seen that the hydrostatic pressure from the gravity tank has a significant effect on the total stresses acting on the acrylic cylinder walls, especially on the 1st filling stage. At the last stage where the pumping pressure was removed, it can be observed that the total stresses acting on the cylinder walls were decreased eventually. After the experiment, laboratory tests were conducted on soils samples from the cylinder. The average bulk unit weight γ_{bulk} of the fill material after the test is 17.9 kPa. With this value, the total pressures acting at TST1, TST2, TST3 and TST4 can be approximated. The calculated total stress based on γ_{bulk} is also plotted in Fig. 13(a) and the ratio between the calculated (reference value) and measured values is plotted in Fig. 13(b). The calculated values for TST3 and TST4 corresponds closely the measured values during the final dewatering stage. There is a substantial difference between the measured and calculated values for TST1 and TST2. One of the possible reason why this has occurred is on how the soil samples at locations Ⓐ and Ⓑ were obtained for the laboratory test. It should be noted that in order to take soil samples at these locations, the cylinder needs to be dismantled at sections ③ and ⑦. It could be that by the time the samples were taken, a sizeable volume of water has already been dissipated. Hence, the calculated values does not account for the dissipated pore water pressure during the soil sampling. The idealized average total stress distribution around the acrylic cylinder's wall is shown in Fig. 14. The total stress element is assumed to be acting normal to the cylinder's surface. The total stress distribution initially illustrates a non-linear behavior during the initial filling stage and linear behavior during the final (stabilized) stage.

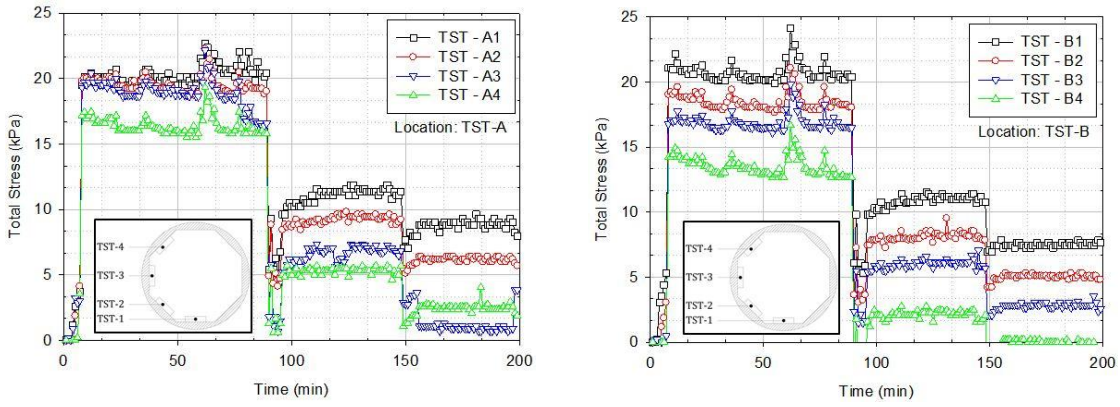

(a) (b)

Fig. 11 Total stress readings for: (a) Model 1; and (b) Model 2

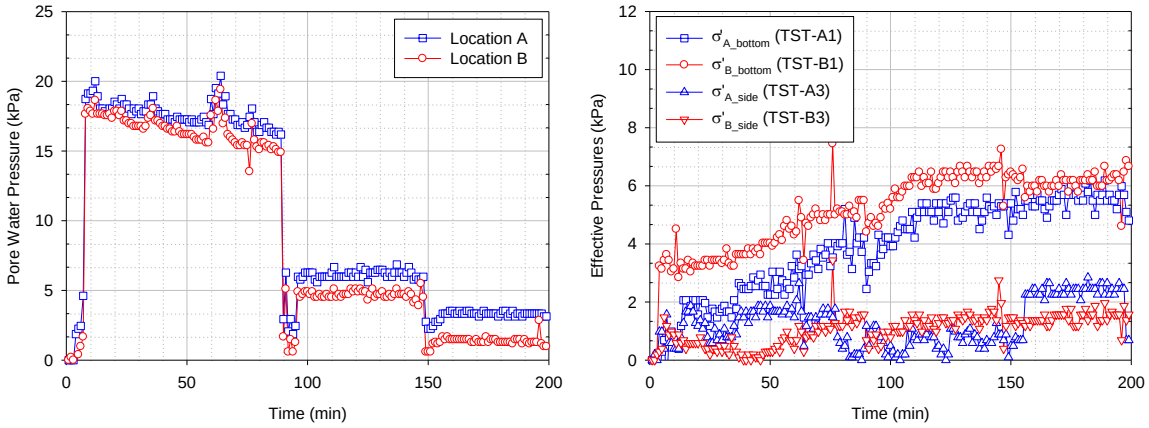

(a) (b)

Fig. 12 (a) Pore water pressure readings at the bottom; and (b) Effective stresses

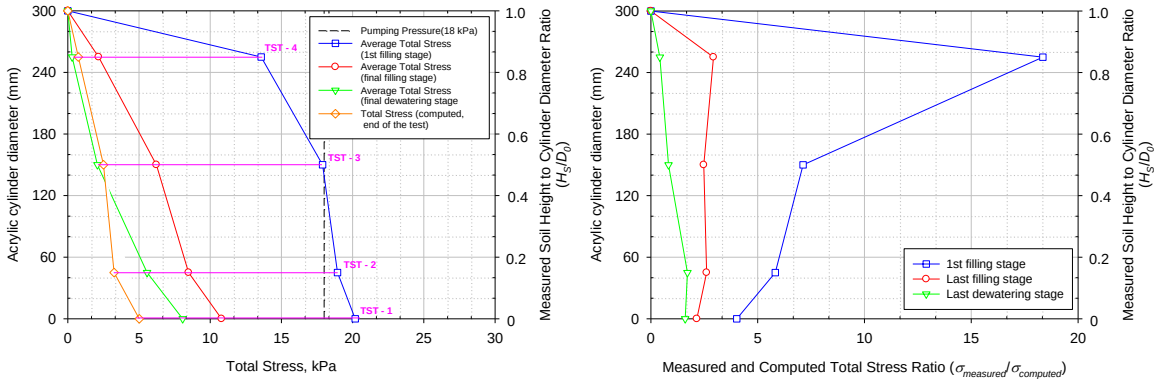

(a) (b)

Fig. 13 (a) Pore water pressure readings at the bottom; and (b) Effective stresses

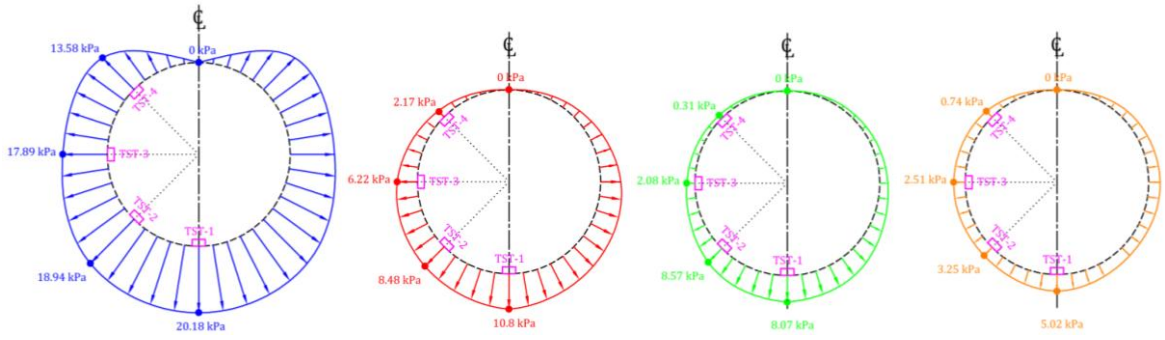

(a) (b) (c) (d)

Fig. 14 Idealized average total stress distribution: (a) Initial filling stage; (b) final filling stage; (c) final dewatering stage, and; (d) calculated total stress at the end of the test

4.2.2 Model 2

The total pressure readings for Model 2 are shown in Fig. 15. The recorded readings for Locations ② (TST-1) and ④ (TST-2) are shown Figs. 15(a) and (c), respectively (please refer to Fig. 7 for the placement of the sensors). Since the sensitivity of the transducers used in this experiment was about 1 kPa, corresponding data based on polynomial curve fitting is provided in Figs. 15(b) and (d) for Locations ② and ④, respectively. Clearly, the pressure readings corresponds to the height of the tube. Interestingly, it appears that the total horizontal pressures (*x* and *y* directions, Fig. 6(c) and Fig. 7) are higher than the total vertical pressures. This phenomenon might be due to the confinement effect of the geotextile sheet to the soil sediments inside the geotextile tube. Presumably, due to the increasing geotextile tensile stress, the soil fills are most likely pushed horizontally (inward direction) rather than vertically as shown in Fig. 16.

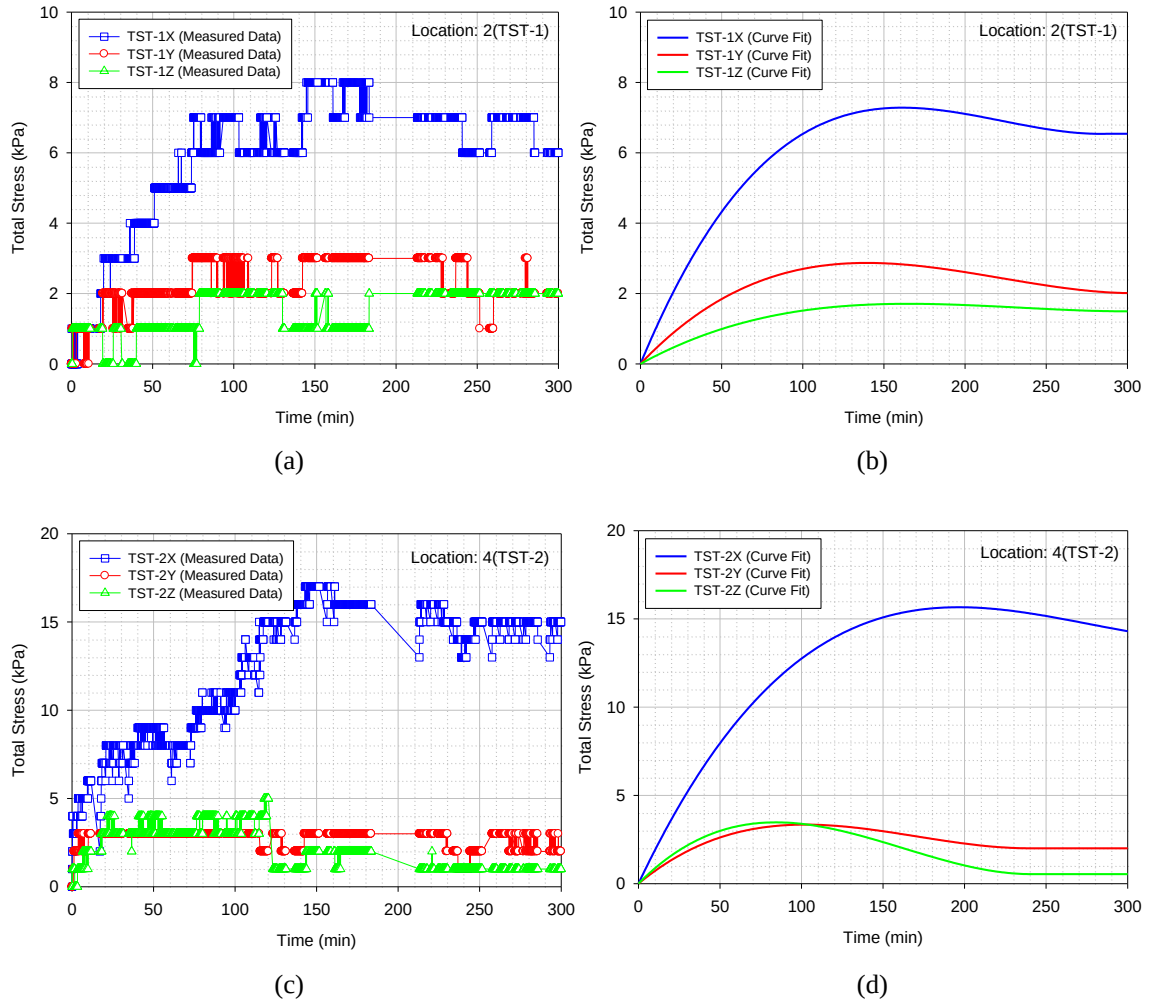

Fig. 15 (a) Total stress readings at Location ②; (b) curve fit for the stress readings at Location ②; (c) total stress readings at Location ④; (d) curve fit for the stress readings at Location ④;

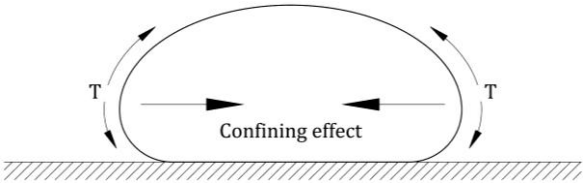

Fig. 16 Geotextile tube's confining effect

In this study, the fill material is assumed to be bounded by a frictionless geotextile membrane. The soil element at any depth in the geotextile tube are subjected to vertical effective pressure, σ'_v, and horizontal effective pressure, σ'_h. The ratio between the effective vertical and horizontal pressures can be defined a non-dimensional K

$$K = \frac{\sigma'_h}{\sigma'_v} \tag{1}$$

The variation in the coefficient of lateral pressures (K) at Locations ② and ④ are shown in Fig. 17. Only the coefficients of lateral pressure corresponding to the time at which measurements for the tube height were taken are plotted. In Fig. 17(a), it appears that coefficient of lateral pressure K of the soil fill at Location ② was increasing during the filling stages and decreased after the last filling stage until it reached steady state. This is reasonable since there was no significant drop in the tube height two days after the last filling stage (refer to Table 3). It might be that the sequence for the lateral earth pressures (total) at Location ② initially began from active state (K_a condition) during filling, passive state (K_p condition) during dewatering and then finally reached steady state (K_0 condition). If this is the case for the soil fill at Location ②, then it suggest that the soil fill at Location ④ was still under active state at time t = 300 min. At this point (t = 300 min), the excess pore water pressure at Location ④ is large compared to the soil deposits at Location ②, which at this point has reached steady state. This is why significant loss in the tube height was observed in Location ④ after two days when it finally achieved steady state.

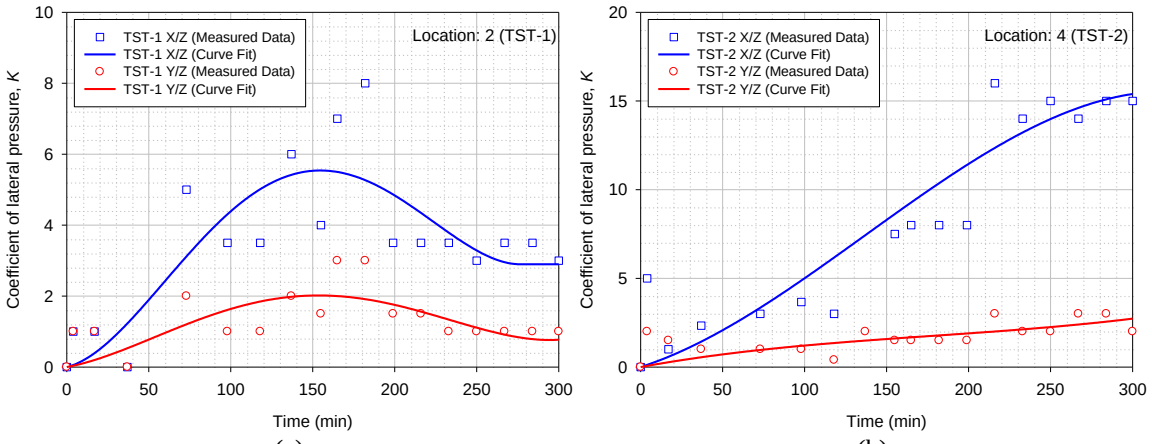

(a) (b)

Fig. 17 Coefficient of lateral pressures at (a) Location ② and (b) Location ④

4.3 Geotextile strain

During the experiment, the strain gauges were oriented along the transverse direction of the geotextile tube to monitor the development of circumferential strain. The data for the geotextile strain at SG-1 and SG-2 (at Locations ② and ④, respectively, as shown in Fig. 7) are shown in Fig. 18. The readings indicates that the geotextile strain increases during the filling process and decreases during the dewatering process. The sharp spikes can be attributed to the effects of the added pumping pressure during filling. Presumably, minimal geotextile strain occurs at the bottom due to the confining effect between the soil fill and foundation. During the test, this assumption is proven accurate as represented by the red line in Figs. 18(a) and (b) for Locations ② and ④. Due to the confinement of the geotextile in-between the fill material (above) and the foundation (below), the geotextile at the bottom of the tube experience only minimal strain during the filling and dewatering process. Another interesting result of the test is the strain readings at the top and sides of the tube. Both strain gauge readings at Locations ② and ④ suggests that the strain at the sides of the tube are larger compared to the strains at the top. This might seem unlikely, however as previously discussed in Section 4.2.2, the magnitude of the total horizontal pressures are larger than the vertical pressures. This implies that the increase in the geotextile strains at the sides of the tube corresponds to the increase in the lateral pressure induced by the fill material.

The existing calculation methods available in the literature assumed that the circumferential tensile force of the geotextile container is constant (Liu and Silvester 1977, Leshchinsky *et al*. 1996, Plaut and Suherman 1998). These assumption was made in order to easily solve the plane strain membrane theory problem. For the present study, the reading for the topmost geotextile strain gauge is significantly low for both geotextile containers and the strain gauge data results shows a variation of strain deformation along its circumference. This suggest that in reality the circumferential tensile forces that causes these deformations are non-uniform along the containers circumferential length. It should be noted that the fill material for the geotextile container considered in the theoretical analysis is fluid. Hence, in the case of the present study, the solidified soil fill may have an influence to the strain variation readings on geotextile tube's circumference.

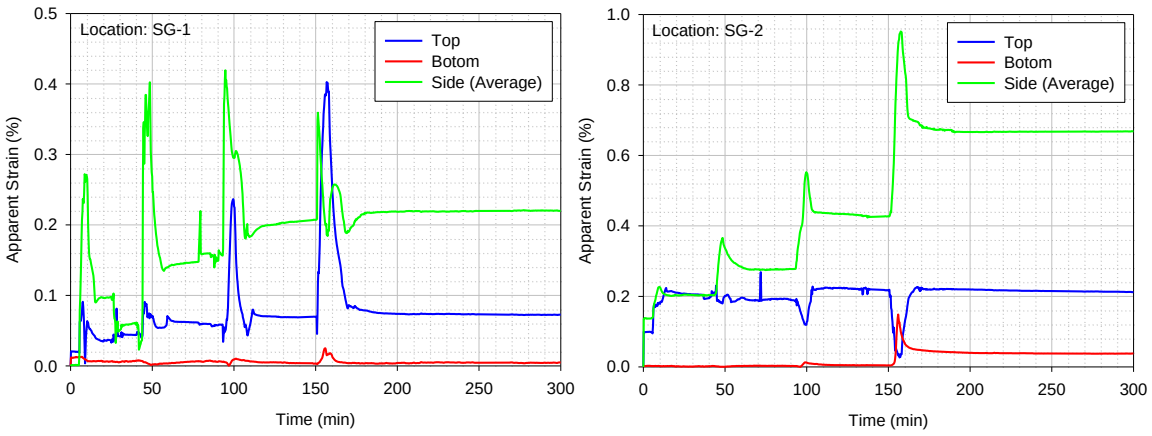

(a) (b)

Fig. 18 Strain readings: (a) Location ② (SG-1) and (b) ④ (SG-2)

5. Conclusions

Based on the laboratory tests conducted, the following conclusions are drawn:

- For rigid containers (Model 1), significant decrease of the sediment height is apparent during the dewatering process. On the other hand, because the geotextile is permeable, the water is gradually dissipated during the filling process of the flexible container (Model 2). Hence, significant loss in the tube height is not apparent during the duration of the test for Model 2.
- Pressure spikes are apparent on rigid containers (Model 1) during the filling process which can be attributed to the confining effect due to hydrostatic pressure. For the flexible containers (Model 2), the pressure readings gradually increases with time during the filling process and normalize at the end on the filling stage. Therefore, the recorded pressures for Model 1 (rigid container) directly corresponds to the hydrostatic pressure while Model 2 (flexible container) directly reflects to the height of the material in the tube.
- Test results indicates that the total horizontal pressures of the material in flexible containers (Model 2) are higher than the total vertical pressures. This phenomenon might be due to the confinement effect of the geotextile sheet to the soil sediments inside the geotextile tube. Presumably, due to the increasing geotextile tensile stress, the soil fills are most likely pushed horizontally (inward direction) rather than vertically.
- Based on the results for Model 2, it is speculated that the sequence for the lateral earth pressures (total) at initially began from active state (K_a condition) during filling, passive state (K_p condition) during dewatering and then finally reached steady state (K_0 condition) after the fill materials stabilized.
- The tangential strain of the geotextile tube (Model 2) varies around its circumference.
- The data readings are at minimal at the bottom of the tube (Model 2). Presumably the stretching of geotextile at these locations are limited due to the confining effect between the soil fill and the foundation.
- The geotextile stains at the sides of the geotextile tube (Model 2) are larger than the geotextile strains at the top. This implies that the increase in the geotextile strains at the sides of the tube corresponds to the increase in the lateral pressure induced by the fill material.
- Due to the variation of the strain distribution on the geotextile (Model 2) skin, the circumferential tensile force of the geotextile may as well be non-constant.

Acknowledgments

This research project is supported by the Technology Advancement Research Program (Grant code: 12TRPI-C064124-01) funded by the Ministry of Land, Infrastructure and Transport in the Republic of Korea.

References

Alvarez, I.E., Rubio, R. and Ricalde, H. (2007), "Beach restoration with geotextile tubes as submerged breakwaters in Yucatan, Mexico", *Geotext. Geomembr.*, **25**(4-5), 233-241.

Brink, N.R., Kim, H.J. and Znidarcic, D. (2015), "Numerical modeling procedures for consolidation of

fine-grained materials in geotextile tubes", *Proceedings of 2015 Geosynthetics Conference*, Portland, OR, USA, February.

Brink, N.R., Kim, H.J. and Znidarcic, D. (2013), "Consolidation modelling for geotextile tubes filled with fine-grained material", *Proceedings of GhIGS GeoAfrica 2013 Conference*, Accra, Ghana, November.

Cantré, S. (2002), "Geotextile tubes–analytical design aspects", *Geotext. Geomembr.*, **20**(5), 305-319.

Cantré, S. and Saathoff, F. (2011), "Design method for geotextile hubes considering strain – Formulation and verification by laboratory tests using photogrammetry", *Geotext. Geomembr.*, **29**(3), 201-210.

Fowler, J., Ortiz, C., Ruiz, N. and Martinez, E. (2002a), "Use of geotubes in Columbia, South America", *Proceedings of the 7th International Conference on Geosynthetics*, Nice, France, September, Volume 3, pp. 1129- 1132.

Fowler, J., Stephens, T., Santiago, M. and De Bruin, P. (2002b), "Amwaj Islands constructed with geotubes, Bahrain", *Proceedings of CEDA Conference*, Denver, CO, USA, pp. 1-14.

Gibeaut, J.C., Hepner, T.L., Waldinger, R., Andrews, J.R., Smyth, R.C., Gutierrez, R., Jackson J.A. and Jackson, K.G. (2003), "Geotubes for temporary erosion control and storm surge protection along the Gulf of Mexico shoreline of Texas", *Proceedings of the 13th Biennial Coastal Zone Conference*, Baltimore, MD, USA, July. [CD-ROM]

Kim, H.J., Lee, K.W., Jo, S.K., Park, T.W. and Jamin, J.C. (2014a), "The influence of filling port system to the accretion and pressure distribution of dredged soil fill in acrylic tubes", *Proceedings of the World Congress on Advances in Civil, Environmental and Materials Research* (*ACEM'14*), Busan, Korea, August. [CD-ROM]

Kim, H., Won, M. and Jamin, J. (2014b), "Finite-element analysis on the stability of geotextile tube-reinforced embankments under scouring", *Int. J. Geomech.* DOI: 10.1061/(ASCE)GM.1943-5622.0000420 , 06014019.

Kim, H.J., Won, M.S., Kim, Y.B., Choi, M.J. and Jamin, J.C. (2014c), "Experimental analysis on composite geotextile tubes hydraulically filled underwater condition", *Proceedings of the World Congress on Advances in Civil, Environmental and Materials Research* (*ACEM'14*), Busan, Korea, August. [CD-ROM]

Kim, H.J., Jamin, J.C. and Mission, J.L. (2013a), "Finite element analysis of ground modification techniques for improved stability of geotubes reinforced reclamation embankments subjected to scouring", *Proceedings of the World Congress on Advances in Structural Engineering and Mechanics* (*ASEM'13*), Jeju, Korea, September, pp. 2970-2979.

Kim, H.J., Jamin, J.C., Won, M.S., Sung, H.J. and Lee, J.B. (2013b), "A study on the behavior of dredged soil stratified in a transparent geobag", *Proceedings of the World Congress on Advances in Structural Engineering and Mechanics* (*ASEM'13*), Jeju, Korea, September, pp. 2980-2987.

Koerner, G.R. and Koerner, R.M. (2006), "Geotextile tube assessment using a hanging bag test", *Geotext. Geomembr.*, **24**(2), 129-137.

Kriel, H.J. (2012), "Hydraulic stability of multi-layered sand-filled geotextile tube breakwaters under wave attack", M.Sc. Thesis; Stellenbosch University, South Africa.

Lawson, C.R. (2008), "Geotextile containment for hydraulic and environmental engineering", *Geosynth. Int.*, **15**(6), 384-427.

Leshchinsky, D., Leshchinsky, O., Ling, H.I. and Gilbert, P.A. (1996), "Geosynthetic tubes for confining pressurized slurry: Some design aspects", *J. Geotech. Eng.*, **122**(8), 682-690.

Liu, G.S. and Silvester, R. (1977), "Sand sausages for beach defence work", *Proceedings of the 6th Australasian Hydraulics and Fluid Mechanics Conference*, Adelaide, Australia, December, pp. 340-343.

Moo-Young, H.K., Gaffney, D.A. and Mo, X. (2002), "Testing procedures to assess the viability of dewatering with geotextile tubes", *Geotext. Geomembr.*, **20**(5), 289-303.

Parab, S.R., Chodankar, D.S., Shirgaunkar, R.M., Fernandes, M., Parab, A.B., Aldonkar, S.S. and Savoikar, P.P. (2011), "Geotubes for beach erosion control in Goa", *Int. J. Earth Sci. Eng.*, **4**, 1013-1016.

Pilarczyk, K.W. (2008), "Alternatives for coastal protection", *J. Water Resour. Environ. Eng.*, **23**, 181-188.

Plaut, R.H. and Klusman, C.R. (1999), "Two-dimensional analysis of stacked geosynthetic tubes on deformable foundations", *Thin-Wall. Struct.*, **34**(3), 179-194.

Plaut, R.H. and Suherman, S. (1998), "Two-dimensional analysis of geosynthetic tubes", *Acta Mech.*, **129**(3-4), 207-218.

Recio, J. and Oumeraci, H. (2009), "Processes affecting the hydraulic stability of coastal revetments made of geotextile sand containers", *Coast. Eng.*, **56**(3), 260-284.

Restall, S.J., Jackson, L.A., Heerten, G. and Hornsey, W.P. (2002), "Case studies showing the growth and development of geotextile sand containers: An australian perspective", *Geotext. Geomembr.*, **20**(5), 321-342.

Weggel, J.R., Dortch, J. and Gaffney, D. (2011), "Analysis of fluid discharge from a hanging bag", *Geotext. Geomembr.*, **29**(1), 65-73.

Vashi, J.M., Desai, A.K. and Solanki, C.H. (2013), "Behavior of geotextile reinforced flyash + clay-mix by laboratory evaluation", *Geomech. Eng.*, **5**(4), 331-342.

JS